Measurements of the thermodynamic equation of state via the pressure dependence of thermophysical properties of air by a thermal-wave resonant cavity

Guang Pan and Andreas Mandelis

Photothermal and Optoelectronic Diagnostics Laboratories (PODL), Department of Mechanical and Industrial Engineering, University of Toronto, 5 King's College Road, Toronto, Ontario M5S 3G8, Canada

The thermodynamic equation of state for ambient air was investigated by means of a thermal-wave resonant cavity in the pressure range between 40 and 760 Torr and at ambient, or near-ambient, temperature conditions. The pressure dependencies of the thermal diffusivity, conductivity, effusivity, and thermal-wave-source infrared emissivity were measured. The experimental results were found to be consistent with the ideal gas law for air in the foregoing pressure and temperature range. It was observed that the thermal diffusivity of air increases linearly with decreasing cavity pressure. The experimental curves obtained from the four channels (amplitude, phase, in-phase, and quadrature) of the thermal-wave signal-demodulating lock-in amplifier were fitted to thermal-wave resonant cavity theory, and the thermal conductivity and effusivity of the air in the cavity were also calculated as functions of pressure. Within the experimental error range, the thermal conductivity was found to be independent of pressure and equal to $(28.9 \pm 0.2) \times 10^{-3}$ W/m K at 309–310 K. The thermal effusivity of air exhibited a linear increase with increasing pressure at approximately constant ambient temperature. In addition, the infrared emissivity of the resistively heated Cr–Ni thermal-wave thin-film strip source (cavity wall) was measured as a function of the source rms voltage at several pressures. The obtained values, ranging from 0.094 to 0.108, showed that the emissivity decreases with decreasing cavity pressure. © *1998 American Institute of Physics.* [S0034-6748(98)01808-5]

I. INTRODUCTION

The thermal-wave resonant cavity (TWRC) has been successfully developed in this laboratory[1] and has found several applications in the measurement of the thermal diffusivity of gases with very high precision and resolution.[2,3] The cavity consists of two parallel walls as shown in Fig. 1. Although conduction heat transfer is a temperature-gradient driven process only and cannot sustain actual energy reflections to form standing waves as is the case with propagating wave fields, the intracavity space supports the *mathematical equivalent* of a standing thermal-wave pattern[1] formed by the rate of coherent thermal oscillation transport across the cavity. The thermal transport rate is thus controlled by local phase relations of the oscillating thermal energy, fixed by the emitting source at one end, and by the presence of the far cavity wall, a coherent thermal resistance or sink, at the other end. This intracavity wall energy confinement can be mathematically described by a standing thermal-wave pattern as a function of intracavity distance.

In our experiments one wall is an electrically resistive thin film element with an ac current generating a surface heat flux at frequency $f = 200$ Hz; the other wall is a polyvinylidene fluoride (PVDF) pyroelectric thin film detector. The PVDF detector produces an ac pyroelectric signal proportional to the amplitude of the effective standing thermal wave between the heater and the detector. By scanning the cavity length L at fixed frequency of the ac current, the thermal diffusivity of the intracavity gas can be measured from the relative distance between adjacent standing thermal-wave extrema in both in-phase (IP) and quadrature (Q) channels of the lock-in amplifier.[1–3] Recently,[3] it was discovered that both conduction and infrared (IR) radiation heat transfer occur simultaneously within the TWRC. A generalized theory for the pyroelectric voltage output has been advanced, taking into consideration both mechanisms.[3] The output ac voltage is given by

$$V(f,L) = \frac{T_a \dfrac{S(f)}{\sigma_p} \left\{ 2b_{gp} \exp(-\sigma_g L) + \dfrac{H}{k_p \sigma_p} [1 - \exp(-2\sigma_g L)] \right\}}{(1 + b_{gp}) - (1 - b_{gp})\exp(-2\sigma_g L)}. \tag{1}$$
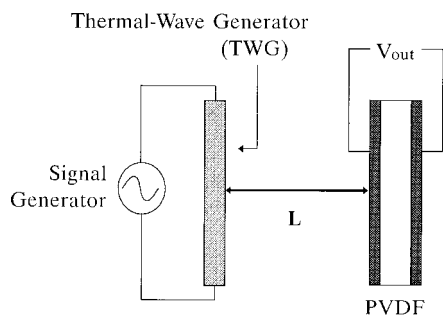
2918   © 1998 American Institute of Physics

FIG. 1. Schematic diagram of the length-scanned thermal-wave resonant cavity.

FIG. 2. Layout of the experimental system, including the TWG metal-strip heater/PVDF transducer cavity and the vacuum pump connections.

Here, T_a is the amplitude of the ac temperature component, $S(f)$ is the instrumental transfer function, a constant for a fixed modulation frequency; b_{gp} is a thermal coupling coefficient at the interface between intracavity gas and PVDF pyroelectric detector; H is a radiation heat-transfer term; σ_g and σ_p are the complex thermal-wave diffusion coefficients of the intracavity gas and PVDF, respectively,

$$H = 4\sigma\epsilon T_{w\mathrm{dc}}{}^3; \quad \sigma_g = (1+i)\sqrt{\pi f/\alpha_g},$$
$$\sigma_p = (1+i)\sqrt{\pi f/\alpha_p}. \tag{2}$$

k_g and k_p denote the thermal conductivity of the intracavity gas and detector, respectively; σ is the Stefan–Bolzmann constant equal to 5.67×10^{-8} W/m^2 K^4; ϵ is the emissivity of the heated surface which emits the infrared radiation; and $T_{w\mathrm{dc}}$ is the dc temperature of the heater. This theory was found to be in excellent agreement with the experimental data of all lock-in amplifier channels (in-phase, quadrature, amplitude, and phase). In the purely conductive mode the H-dependent term in Eq. (1) is absent and the thermal coupling coefficient b_{gp} must be evaluated from the expression in the denominator of $V(f,L)$, since its presence in the numerator amounts to a simple shift of the amplitude of the signal, which cannot be easily quantified. The reliable estimation of this parameter is, however, very difficult because it is usually much smaller than one ($\sim 10^{-2}$–10^{-3} for gas–solid interfaces). The existence of the radiation mode offers the unique opportunity to accurately measure the value of b_{gp} by adjusting the cavity length L to distances such that the b_{gp}—proportional exponentially decaying conductive (first) term in the numerator of $V(f,L)$ becomes of the same order of magnitude as the radiation (second) term which is driven to saturation at large L. Thus, based on the definitions (2) and on

$$b_{gp} = k_g \sqrt{\alpha_p}/k_p \sqrt{\alpha_g}, \tag{3}$$

it becomes possible to reliably obtain the thermal conductivity of the intracavity gas as well as the emissivity of the thin-film heater from direct measurements of b_{gp} and H, by fitting the generalized theory to experimental data. Furthermore, the measurement of the thermal diffusivity and conductivity of the gas allows the calculation of its thermal effusivity and its density (if the specific heat at constant volume is known) as indirect measurements. Therefore, this methodology can be used to study the thermodynamic equation of state for a given gas by means of the dependence of
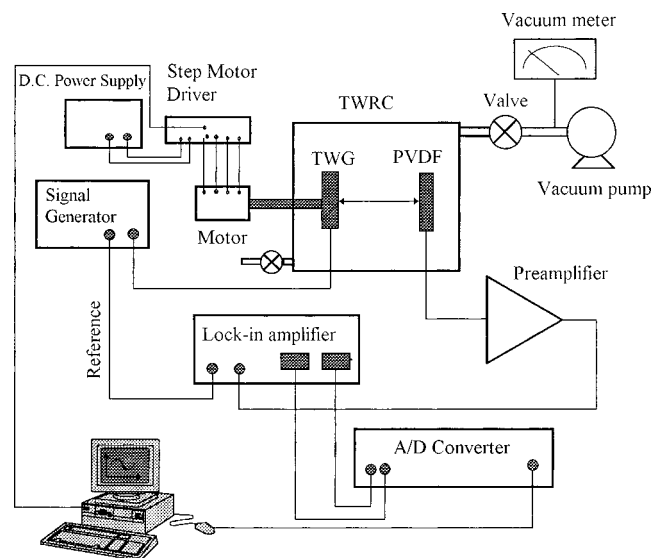
the foregoing thermophysical properties on the intensive thermodynamic parameters of the system (pressure, temperature) taking advantage of the high precision measurements of the primary quantities (thermal diffusivity and conductivity) afforded by the TWRC. In the present work, the thermodynamic behavior of the intracavity gas as a function of pressure was investigated for the first time using the TWRC as an extension of our earlier static (isobaric) study.[3]

II. INSTRUMENTATION AND EXPERIMENT

Figure 2 shows the layout of the experimental setup used to perform pressure dependent measurements between 760 and 40 Torr. The thermal-wave generator (TWG) refers to the Cr–Ni thin-film strip resistive heater that generates a Joule-effect thermal wave due to the flowing ac current following the application of an ac voltage waveform from a synthesized function generator (Stanford Research Systems model DS335). The TWG is mounted on a micrometer stage, which is driven by a computer-controlled dc step motor, allowing a 10 μm resolution in scanning cavity length. The electrical signal at the PVDF pyroelectric detector induced by the thermal wave is amplified by a preamplifier (ITHACO model 1201), followed by further amplification and demodulation by a lock-in amplifier (EG&G model 5204). Data acquision is facilitated with a personal computer connected to the lock-in amplifier through an analog-to-digital converter. The TWRC is placed in an enclosed chamber which provides a thermodynamically controlled environment to yield equilibrium measurements of the values of the thermophysical properties of the intracavity air. For the low-pressure measurements, a vacuum pump was connected to the chamber. The air pressure within the chamber was adjusted by a valve between the vacuum pump and the chamber. The minimum chamber pressure that can be reached under the current chamber design is 40 Torr. A vacuum gauge (Leybold CM-330) with a dc voltage output at the rear terminals was used to monitor air pressure. Since the readable pressure range in the vacuum meter was narrow, a nonlinear calibration curve
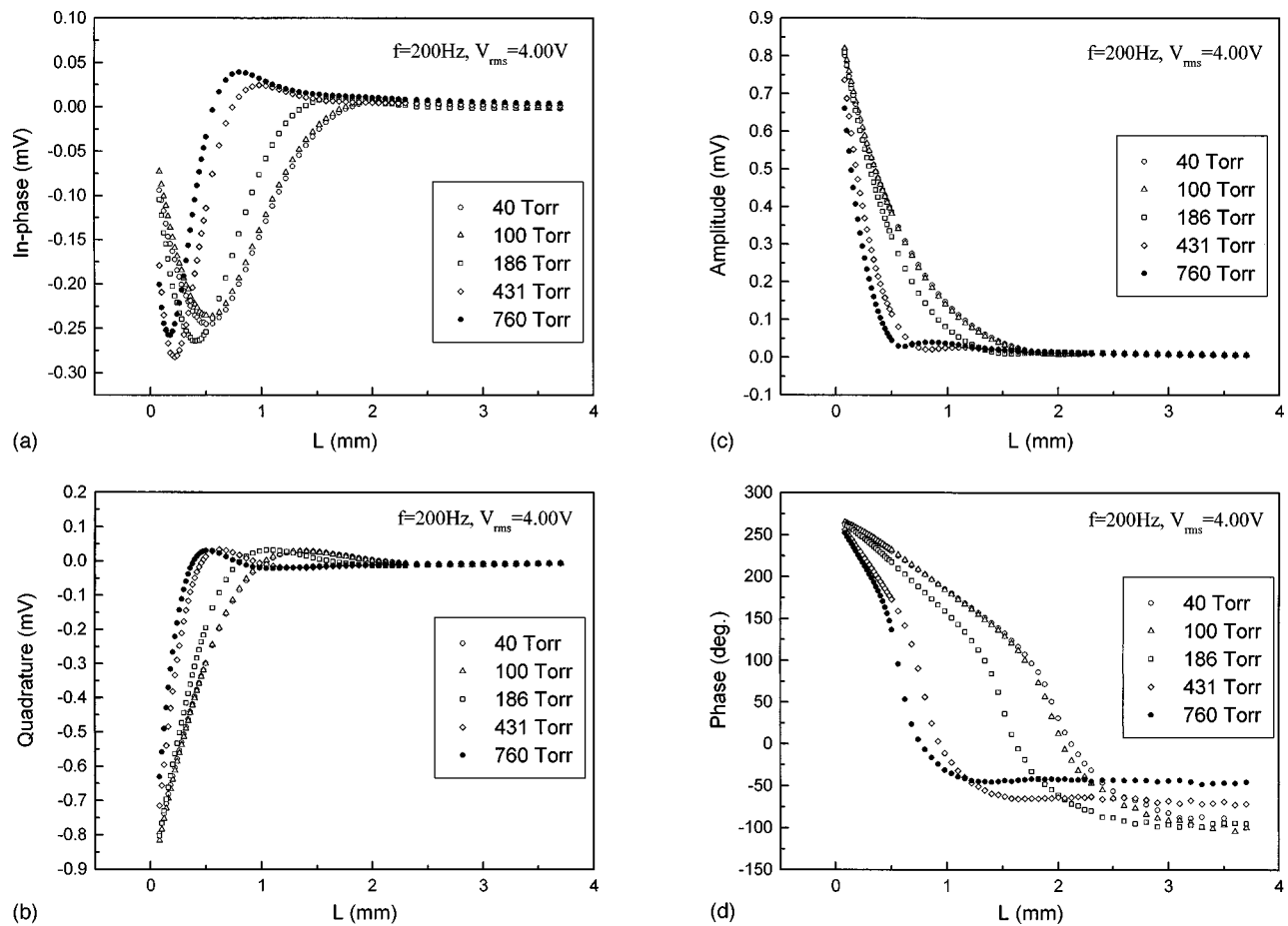
FIG. 3. Demodulated lock-in amplifier signal outputs at various TWRC pressures. (a) In-phase, (b) quadrature, (c) amplitude, and (d) phase channel.

was generated between the vacuum gauge meter readout and the higher resolution output voltage at the rear panel terminals. By interpolating the calibration curve, output voltages corresponding to the pressure range between 40 and 760 Torr could be obtained with reasonable accuracy. The experimental pressure between 40 and 760 Torr could be controlled through the valve and by monitoring the output voltage of the vacuum gauge. The room air in the relative humidity range of 22–35% at 25 °C was used as a sample gas. Cavity length scans were conducted at 200 Hz. For the low-pressure measurements, data collection started after the chamber pressure attained a stable value. To measure the IR emissivity of the Cr–Ni thin-film heater as a function of pressure using the previously reported method,[3] the ac V_{rms} voltage applied across the heater was varied from 1.50 to 5.00 V.

III. RESULTS AND DISCUSSION

The thermal-wave cavity-length-scanned signals measured as a function of ambient air pressure via the four lock-in amplifier channels are shown in Fig. 3. For the purpose of comparisons in the phase channel, which is the one most affected by the presence of the radiation heat transfer mode in the cavity,[3] the initial phases for various chamber pressures were adjusted to (roughly) the same value before the onset of the measurement, Fig. 3(d). The resonant peaks in the in-phase curve, Fig. 3(a), are broadened significantly with decreasing chamber pressure, indicating a substantial

increase in the thermal diffusivity of the gas. Saturation appears to set in at pressures below 100 Torr. Similar trends are evident in the quadrature channel, Fig. 3(b). The amplitude also varies with pressure, especially at short cavity lengths ($\sim$ one thermal diffusion length). For fixed cavity length, the amplitude was observed to increase with decreasing pressure, indicating an increase in signal intensity consistent with enhanced thermal transport across the cavity gap. In Fig. 3(c) the amplitudes have been normalized to the value of the shortest cavity length at the lowest pressure (40 Torr). The signal saturation with cavity length at pressures below 100 Torr is observed in all four signal channels. Furthermore, three channels (with the exception of phase) exhibit signal decay to zero level at cavity lengths long compared to the thermal diffusion length, as expected from conduction-dominated transport. On the other hand, the phase, Fig. 3(d), is the only channel exhibiting enhanced sensitivity to the nonconduction mechanism operating in the cavity-length range beyond the thermal diffusion length at each pressure. This mechanism was shown to be due to radiation heat transfer upon domination of the phase of the complex pyroelectric voltage $V(f,L)$ by the second term in the numerator of Eq. (1).[3] With decreasing pressure, the onset of the flat portion of the phase curve corresponding to radiation contribution to heat transfer shifts to a longer cavity length commensurate with the spatially expanded domination of conduction heat transfer due to the increased diffusivity (and thermal diffu-
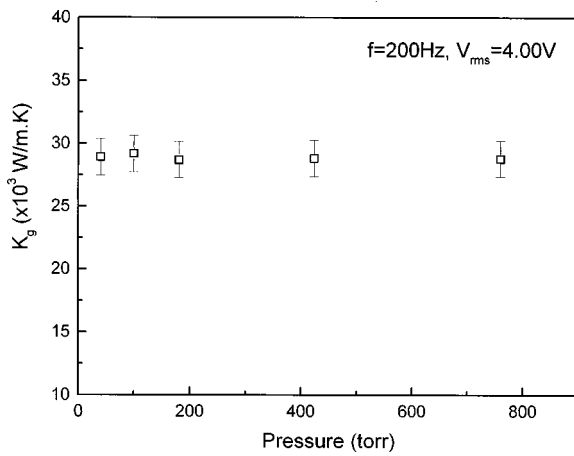
FIG. 4. Thermal conductivity of intracavity air as a function of pressure.

FIG. 5. Inverse of measured thermal diffusivity of the intracavity air as a function of pressure.

sion length) in the intracavity region. The strengthening of conductive transfer with decreasing pressure is accompanied by proportionately weakened radiative transport, presumably due to the decrease of the absolute temperature of the source, as the heat-load reducing thermal diffusivity of the gas surrounding the metallic strip increases.

The thermal conductivity of the intracavity gas was obtained from the thermal coupling coefficient b_{gp}, Eq. (3). Under the small temperature variations of the experiments, k_p and α_p of the PVDF detector were taken as constants. The generalized theoretical expression, Eq. (1), was fitted to the experimental curves of Figs. 3(a)–3(d) using the method of least squares. Thus both thermal diffusivity and b_{gp} were measured as fitting parameters. The thermal diffusivity of the intracavity air was measured from the in-phase signal using the relative distance between two consecutive extrema (the first: minimum, and the second: maximum)[3] at each pressure in the data of Fig. 3(a).

Figure 4 shows the thermal conductivity of intracavity air as a function of pressure as calculated from Eqs. (1) and (3) with the value of α_g inserted from the foregoing diffusivity measurements, and the value of b_{gp} derived by a least-squares fit of the theory to the experimental phase data. It can be seen that within the experimental error range, the thermal conductivity of intracavity air is independent of pressure, as expected from the kinetic theory of gases in the investigated pressure range.[4] The calculated value of thermal conductivity, $(28.9 \pm 0.2) \times 10^{-3}$ W/m K, is higher than the literature value[5] of 26.3×10^{-3} W/m K at 300 K. This can be attributed to the rise in intracavity air temperature above its room value. The average temperature of the intracavity air can be calculated from the generalized theory[3] provided the surface temperature of the heater and ambient temperature, T_∞, are known. Using a contacting thermocouple, the temperature of the heater surface was measured at various pressures. The measurement gave a value of 321 K at 760 Torr while for 100 and 40 Torr the surface temperature of the heater was 318 K. The small decrease was probably caused by the increase in ambient thermal diffusivity. From these surface temperatures and other known parameters of the cavity, the average intracavity air temperature was calculated to be 308–309 K. The thermal diffusivity calculated from the in-
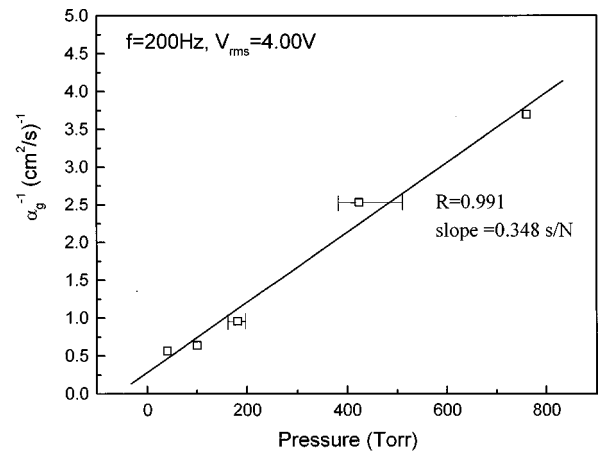
phase curve extrema was found to be inversely proportional to the pressure within the experimental error range, Fig. 5. The unequal and asymmetric horizontal error bars shown in that figure are estimates of uncertainties in the extrapolated calibration curve used to measure the chamber pressure in the intermediate experimental range of this work (200–600 Torr). These uncertainties have limited the accuracy of the thermal-diffusivity measurements to two significant figures, instead of the four-significant-figure accuracy, of which the TWRC is capable.[3] Gas thermal diffusivity is related to primary thermophysical parameters by

$$\alpha_g \equiv \frac{k_g}{\rho C_p}, \qquad (4)$$

where k_g is the thermal conductivity; ρ is the density; and C_p is the constant-pressure specific heat. Given that the specific heat is associated with the total internal energy of the gas and is a function of temperature only, it can be assumed constant under the present experimental conditions. Since the thermal conductivity of air was found not to depend on pressure, Fig. 4, it can be expected that thermal diffusivity should be consistently inversely proportional to both density and pressure, *only* if the cavity air can be treated as an ideal gas. The slope of the best-fit straight line in Fig. 5 is 0.00463 s/cm² Torr (0.348 s/N in MKS units). Under the assumption of an ideal gas, the pressure in the chamber can be expressed as

$$P = \frac{\rho R T}{M}, \qquad (5)$$

where R is the universal gas constant and M is the molar mass of the gas. From Eqs. (4) and (5),

$$\frac{d}{dP}(\alpha_g^{-1}) = \frac{d}{dP}\left(\frac{\rho C_p}{k_g}\right) = \frac{d}{dP}\left(\frac{C_p PM}{k_g RT}\right) = \frac{C_p M}{k_g RT}. \qquad (6)$$

Substituting $M = 28.8 \times 10^{-3}$ kg/mole (average molar mass of air),[5] $C_p = 1.006$ kJ/kg °C,[6] $R = 8.314$ J/mole K, $T = 309$ K, and $k_g = 28.9 \times 10^{-3}$ W/m K,[5] Eq. (6) yields a $d(\alpha_g^{-1})/dP$ value of 0.394 s/N. This is in reasonable agreement with the slope value obtained from the linear fit in Fig. 5, in view of the uncertainties in absolute pressure values.
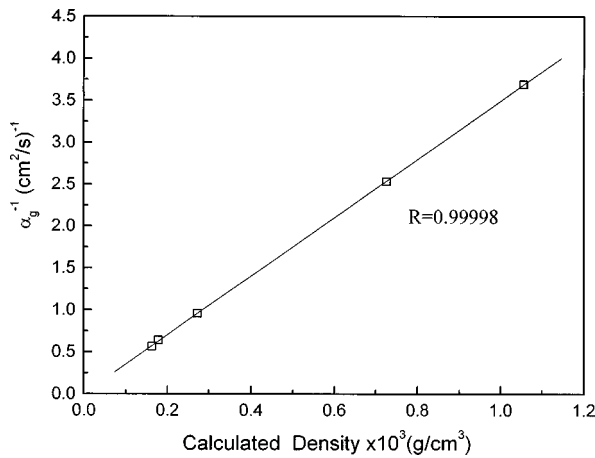
FIG. 6. Inverse of thermal diffusivity of the intracavity air vs density calculated from the measured values of diffusivity and conductivity at various cavity pressures.

FIG. 7. Square of the thermal effusivity of intracavity air as a function of pressure.

Equation (4) indicates that a plot of the inverse of the thermal diffusivity α_g vs gas density should be linear. This was checked independently of the experiments that produced Fig. (5). A relatively low ac voltage across the thermal-wave source was used, so as to keep the intracavity gas temperature nearly constant, and the intracavity gas density close to that of the surrounding air throughout a series of experiments at different pressures. The thermal diffusivities, $\alpha_g(P)$, were calculated from the adjacent in-phase channel extrema. The thermal conductivities, $k_g(P)$, were calculated from values of the coefficient $b_{gP}(P)$ as shown in Fig. 4. Then densities $\rho(P)$ were calculated from Eq. (4). The results are plotted in Fig. 6, which shows an excellent linear relation between α_g^{-1} and ρ with a correlation coefficient $R=0.99998$. The better linear fit of the plot in Fig. 6 compared to that in Fig. 5 is due to the fact that the (α_g, ρ_g) data pairs in the former were generated simultaneously at a single pressure (α_g: measured; ρ_g: calculated) and no knowledge of the precision-limiting absolute value of the pressure was required. The coexistence of the linear relations of Figs. 5 and 6 implied $\rho_g \propto P$ and is consistent with the underlying assumption that the intracavity air can be treated as an ideal gas in the investigated experimental pressure range. Under general experimental conditions, the TWRC measurement of $\rho(P)$ or $\rho(T)$ of a gas from its thermal diffusivity and conductivity values via Eqs. (1), (3), and (4) can determine one or more thermodynamic equations of state for the gas.

In addition to the TWRC measurements of the foregoing thermophysical parameters and the determination of the equation of state for a gas, the measurement of its thermal effusivity, an important thermophysical property involved in interfacial thermal transport between material phases, can be derived from Eqs. (3) and (4):

$$e_g = \sqrt{k_g \rho C_p} = \frac{k_g}{\sqrt{\alpha_g}}. \tag{7}$$

As a result of the fact that the thermal conductivity k_g was found not to change with pressure and the thermal diffusivity was inversely proportional to the pressure, the square of the thermal effusivity is predicted to be proportional to pressure.
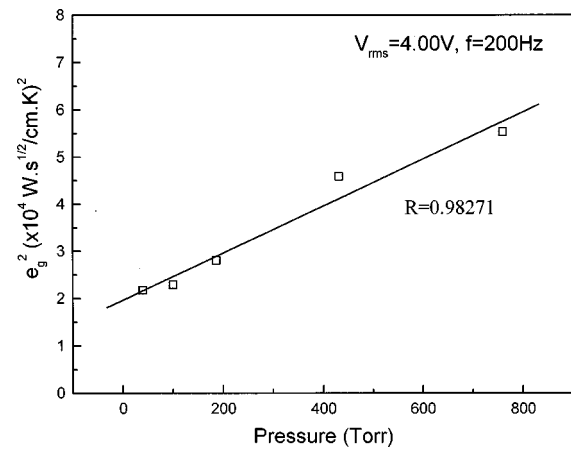
Figure 7 was constructed from experimental TWRC data for α_g and k_g as functions of gas pressure. It can be seen that the absolute value of $e_g(P)$ can be measured and there exists a linear relationship between the square of effusivity and pressure, as expected. The measured effusivity of air at 760 Torr and 310 K ($V_{rms}=4.0$ V) was found to be (5.54 ± 0.01) W s$^{1/2}$/m^2 K, in good agreement with the literature value of 4.7 W s$^{1/2}$/m^2 K at 300 K.[7]

A simple methodology has been reported[3] for measuring the absolute value of the infrared emissivity, ϵ, of the Cr–Ni strip thin-film heater by varying the ac voltage applied to the heater and fitting the thermal-wave phase data to the theory, Eq. (1), along with known values of α_g, to obtain the value of $H(V_{ac})$. By plotting H vs the square of the ac voltage and fitting the curve to a cubic function, the emissivity of the heater can be found from the $V_{rms}=0$ intercept[3] using the expression for H from Eq. (2) with $T_{wdc}=T_\infty$. The results are shown in Fig. 8. The emissivity of the Cr–Ni thin-film strip heater demonstrated a tendency to decrease with decreasing chamber pressure. This was most likely caused by the increased thermal diffusivity of the intracavity air, which, in turn induced a decrease in the average dc temperature of the thermal-wave source, as verified by the contacting ther-
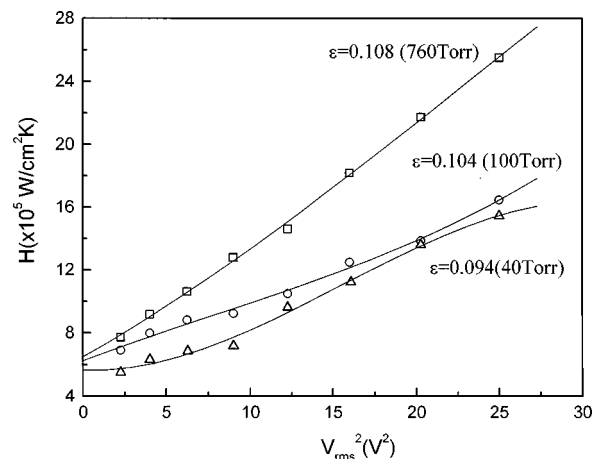

FIG. 8. Radiation heat-transfer coefficient H as a function of the square of the rms value of the applied V_{ac}.

TABLE I. Comparison of TWRC experimental values for air at 760 Torr with literature values.

	$\alpha_g\, 10^6 (\text{m}^2/\text{s})$	$k_{gx} 10^3$ (W/m K)	ρ (kg/m^3)	e_g (W s$^{1/2}$/m^2 K)
Literature value (at 300 K)	22.5[a]	26.3[a]	1.1614[a]	4.7[b]
Literature value (at 350 K)	29.9[a]	30.0[a]	0.9950[a]	
Experimental value (at 309–310 K)	27.06±0.06	28.9±0.2	1.057±0.005	5.54±0.01

[a]Reference 8.
[b]Reference 7.

mocouple. The emissivity value at 760 Torr was 0.108, which is slightly higher than that reported earlier[3] for the same heater (0.091±0.004). This is probably due to chemical changes of the metallic surface caused by oxidation following the continuous usage of the TWRC and exposure of the heater to ambient conditions. Table I lists experimental thermophysical values for air obtained in the present experiments at 760 Torr. It can be seen from the literature values provided in Table I that the experimental values are in close agreement to the literature values.

A thermal-wave resonant cavity was used to determine the thermodynamic equation of state of air under ambient temperature (309–310 K) in the pressure range 40–760 Torr. The TWRC was used to measure the thermal diffusivity, conductivity, effusivity, and density of air in the same pressure range. In separate experiments it was found that the thermal diffusivity was inversely proportional to gas pressure and gas density across the examined pressure range, thus proving that air obeys the ideal gas law. When the pressure changed from 760 to 40 Torr, the thermal diffusivity increased from 2.70×10^{-5} to 17.6×10^{-5} m^2/s. The thermal conductivity was found to be independent of the gas pressure with an average value of $(28.9 \pm 0.2) \times 10^{-3}$ W/m K, in agreement with predictions from the kinetic theory of gases. The pressure dependence of the thermal effusivity of air was further obtained as a derivative quantity from the measured thermal diffusivity and conductivity. The square of the effusivity was found to increase linearly with pressure, in agree-

ment with the ideal gas equation of state. The infrared emissivity of the thin-metallic-film thermal-wave source was found to decrease as the pressure decreased, consistent with a decreased average heater temperature. In conclusion, the TWRC has been shown to be an effective precision device for the determination of the thermodynamic equation state of gaseous matter by means of the measurement of the thermophysical properties of gases.

ACKNOWLEDGMENTS

[1] J. Shen and A. Mandelis, Rev. Sci. Instrum. **66**, 4999 (1995).
[2] J. Shen, A. Mandelis, and D. Aloysius, Int. J. Thermophys. **17**, 1241 (1996).
[3] J. Shen, A. Mandelis, and H. Tsai, Rev. Sci. Instrum. **69**, 197 (1998).
[4] E. H. Kennard, *Kinetic Theory of Gases with an Introduction to Statistical Mechanics* (McGraw–Hill, New York, 1938).
[5] D. Halliday and R. Resnick, *Fundamentals of Physics*, Extended 2nd ed. (Wiley, New York, 1981), Chap. 21.
[6] A. Rosencwaig, *Photoacoustics and Photoacoustic Spectroscopy* (Wiley, New York, 1980), p. 96.
[7] G. Busse and H. G. Walther, in *Principles and Perspectives of Photothermal and Photoacoustic Phenomena*, edited by A. Mandelis (Elsevier, New York, 1992), Vol. 1, p. 218.
[8] F. P. Incopera and D. P. Dewitt, *Fundamental Heat and Mass Transfer*, 3rd ed. (Wiley, New York, 1990).